Effect of a floating electrode on a plasma jet

J. T. Hu, J. G. Wang, X. Y. Liu, D. W. Liu, X. P. Lu, J. J. Shi, and K. Ostrikov

Citation: Physics of Plasmas (1994-present) **20**, 083516 (2013); doi: 10.1063/1.4817954
View online: http://dx.doi.org/10.1063/1.4817954
View Table of Contents: http://scitation.aip.org/content/aip/journal/pop/20/8?ver=pdfcov
Published by the AIP Publishing

Effect of a floating electrode on a plasma jet

J. T. Hu,[1] J. G. Wang,[1] X. Y. Liu,[1] D. W. Liu,[1,a)] X. P. Lu,[1] J. J. Shi,[2] and K. Ostrikov[3]
[1]*State Key Laboratory of Advanced Electromagnetic Engineering and Technology, Huazhong University of Science and Technology, WuHan, HuBei 430074, People's Republic of China*
[2]*College of Science, Donghua University, Shanghai 201620, People's Republic of China*
[3]*Plasma Nanoscience Centre Australia (PNCA), CSIRO Materials Science and Engineering, P. O. Box 218, Lindfield, New South Wales 2070, Australia*

(Received 23 May 2013; accepted 22 July 2013; published online 29 August 2013)

Two kinds of floating electrode, floating dielectric barrier covered electrode (FDBCE) and floating pin electrode (FPE), which can enhance the performance of plasma jet are reported. The intense discharge between the floating electrode and power electrode decreased the voltage to trigger the plasma jet substantially. The transition of plasma bullet from ring shape to disk shape in the high helium concentration region happened when the floating electrode was totally inside the powered ring electrode. The enhanced electric field between propagating plasma bullet and ground electrode is the reason for this transition. The double plasma bullets happened when part of the FDBCE was outside the powered ring electrode, which is attributed to the structure and surface charge of FDBCE. As part of the FPE was outside the powered ring electrode, the return stroke resulted in a single intensified plasma channel between FPE and ground electrode. © *2013 AIP Publishing LLC*.
[http://dx.doi.org/10.1063/1.4817954]

I. INTRODUCTION

The term *floating electrodes* means metallic objects that are disconnected from the ground, which are used widely in lighting protection system.[1] Recently, the floating electrodes are introduced into gas plasma sources development to improve their performances.[2–4] A pair of pin electrodes consist of one floating electrode and one powered electrode effectively increased the plasma plume length,[5] and a floating electrode separated from main electrodes by a slim dielectric barrier decreased the ignition voltage of non-thermal arc discharges significantly.[6] However, there are surprisingly few reports on the effect of different materials which make up floating electrode and the various distance between power electrode and floating electrodes. In this paper, we shall report the performance of the plasma sources affected by the floating dielectric barrier covered electrode and floating stainless steel pin electrode, and various distance between the power electrode and floating electrodes.

II. EXPERIMENT SETUP

The plasma jet used for this study is shown schematically in Fig. 1, with a ring power electrode wrapped around the quartz tube near the tube nozzle and a floating electrode recessed within the quartz tube. The inner diameter and outer diameter of the quartz tube were 8 mm and 10 mm, respectively. Two kinds of floating electrode were used, one is stainless steel pin of accurately machined radius of curvature (20 μm) and the other one is a slim glass tube (inner diameter of 4 mm) with slim copper wire inside and one sealing end.[7,8] The floating electrode is placed at two positions as shown in Fig. 1, one is inside the tube and the horizontal distance between the floating electrode and the power electrode is 5 mm (Fig. 1(a)), and the other is that part of the floating electrode (5 mm) is out of the quartz tube (Fig. 1(b)). The ring electrode is powered by a pulsed DC voltage (amplitudes up to 10 kV, repetition rate is 10 kHz, and pulse width is 300 ns). An indium tin oxide (ITO) ground electrode was placed 2 cm downstream from the quartz tube nozzle, with its ITO covered side towards the plasma jets. Helium (99.996%) was used as carrier gas and the gas flow rate is 5 slm. Voltage and current signals were measured with Tektronix P6015AS 75 MHz high voltage probe and a Pearson 2877 1 V/1 A 200 MHz current probe, respectively, and recorded via a Tektronix DPO4104 oscilloscope (1 GHz bandwidth and 10 mega-bit sample record length). Plasma images were taken by the digital camera Nikon D700 and ICCD camera (Princeton Instruments, PIMAX2).

III. EXPERIMENT RESULT AND DISCUSSION

When the floating dielectric barrier covered electrode (FDBCE) was inside the tube, the gas breakdown happened at the pulsed DC voltage of 5.02 kV, and the plasma extended out of the tube for 0.7 cm as shown in Fig. 2(a). The breakdown voltage decreased to 3.7 kV when part of the FDBCE was moved out of the tube for 5 mm; this is attributed to the decreased gap distance between the FDBCE and the power electrode [Fig. 2(c)]. Without the dielectric barrier, the pin electrode is expected to decrease the breakdown voltage,[9] and this indeed happened for the case of the floating pin electrode (FPE) outside tube. Its breakdown voltage was 3.2 kV, and most of the plasma was confined inside the tube [Fig. 2(d)]. However, when the pin electrode was inside the tube, the breakdown voltage was 5.6 kV, which was 62% higher than the voltage of FDBCE inside tube. Such a high breakdown voltage not only initialized the intense discharge inside the tube but also extended the plasma to the ground electrode

a)Author to whom correspondence should be addressed. Electronic mail: liudw@hust.edu.cn

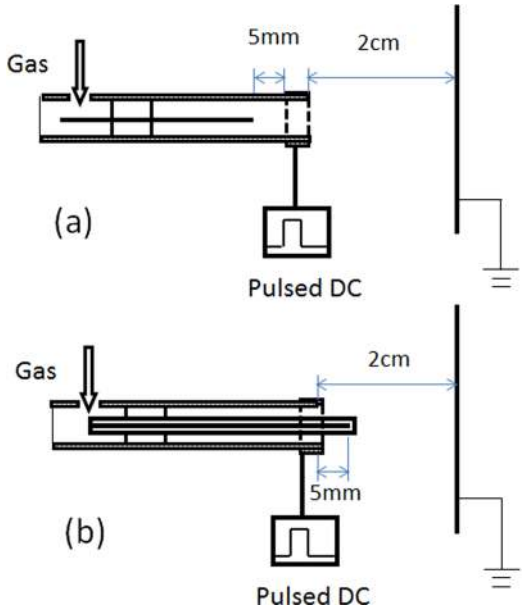

FIG. 1. Schematic of plasma jet with floating electrode. (a) Floating electrode (pin electrode) is totally inside the tube. (b) Part of the floating electrode (dielectric barrier covered electrode) is out of the tube.

[Fig. 2(b)]. On the other hand, the case without floating electrode was also tested. As the pulsed DC voltage was increased to 10 kV (maximum output of the power supply) and the gap between power electrode and ground electrode was decreased to 1 cm, the plasma did not arise (image not shown), which proved ability of the floating electrode to decrease the voltage initialize the discharge.

Fig. 3 shows pictures of the plasma jets with the same setup as four cases in Fig. 2, when the pulsed DC voltage (V_{PD}) was increased to 6 kV. Because the exposure time of pictures in Figs. 2 and 3 was fixed at 0.4 s, the comparison between Figs. 2 and 3 with FDBCE and FPE at same position shows the difference of the plasma jet intensity. The higher V_{PD} increased the power coupled to plasma; therefore, the plasma jet became longer and brighter [compare Figs. 3 and 2]. For the cases of floating electrode inside the tube, Fig. 3(b) shows the stronger plasma jet of the FPE than that of the FDBCE, which is attributed to more power consumed by the discharge inside the tube of the FDBCE [Fig. 3(a)]. For the case of part of floating electrode outside the tube, the double stream from the end of the FDBCE [Fig. 3(c)] make the plasma jet wider than the other cases, and the single intensified plasma jet from the FPE was

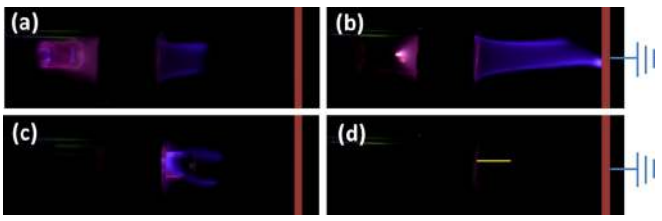

FIG. 2. Images of a plasma jet arising with FDBCE and FPE at different positions: (a) FDBCE inside the tube, $V_{PD} = 5.02$ kV; (b) FPE inside the tube, $V_{PD} = 5.6$ kV; (c) FDBCE outside the tube, $V_{PD} = 3.7$ kV; (d) FPE (yellow line) outside the tube, $V_{PD} = 3.2$ kV. The exposure time of each picture is 0.4 s.

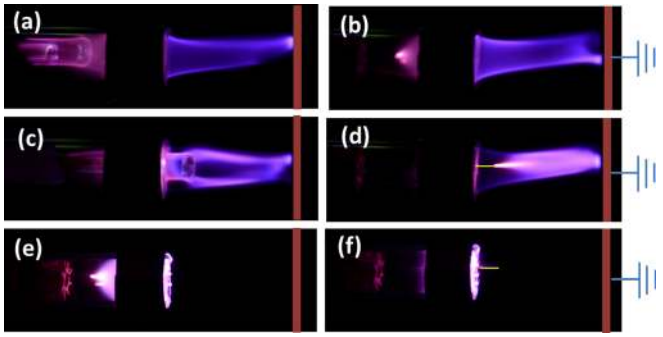

FIG. 3. Images of a plasma jet arising with FDBCE and FPE at different positions: (a) FDBCE inside the tube; (b) FPE inside the tube; (c) FDBCE outside the tube; (d) FPE (yellow line) outside the tube. The pin electrode connected with ground when (e) pin electrode inside the tube and (f) pin electrode outside the tube. $V_{PD} = 6$ kV. The exposure time of each picture is 0.4 s.

observed in Fig. 3(d)]. On the other hand, although the ground connected pin electrode initiated much more intense discharge [Figs. 3(e) and 3(f)], most of the plasma is confined inside the tube due to the strong cross direction electric field[10] between the power electrode and the ground pin electrode.

Plasma jets are known to be affected by the helium mole fraction along the plasma jet propagation path;[11] therefore, computational fluid dynamics simulation to characterize helium mole fraction and helium velocity in the experiment region was performed by COMSOL Multiphysics 4.3. The governing equations consist of Navier-Stokes, continuity, and convection-diffusion equations. The inlet helium flow rate from the bottom opening of the tube is 5 SLM, and the air inlet velocity adjacent to the opening of tube is 2%[11] of the helium inlet velocity. Fig. 4 shows the helium mole fraction from the tube exit to the ground electrode with FDBCE and FPE at different positions. The helium mole fraction is almost 1 in the column along the tube exit for all cases because the short distance to the ground electrode compared with cases reported in Refs. 11 and 12.

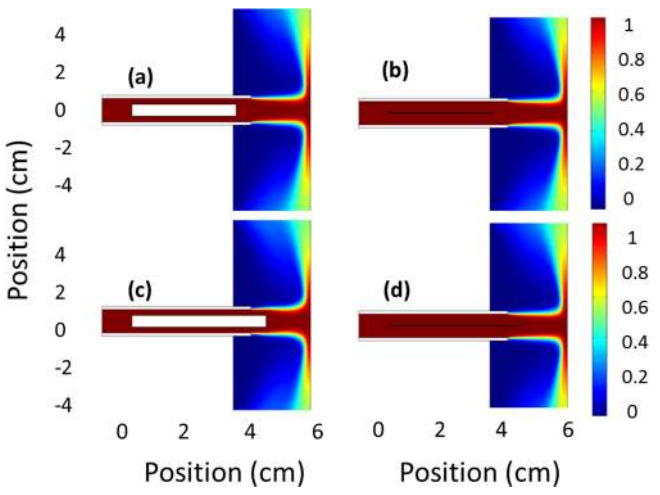

FIG. 4. Helium mole fraction within the tube and between the tube and ground electrode as a function of radial and axial directions for helium flow rate of 5 SLM: (a) FDBCE inside the tube; (b) FPE inside the tube; (c) FDBCE outside the tube; (d) FPE outside the tube.

Fig. 5(a) shows the temporal characteristics of the applied voltage on the ring electrode and the induced voltage on the floating electrodes. During the rising phase of the applied pulse voltage (before the gas breakdown inside the tube), the floating electrode worked as a voltage probe inside the strong electric field; therefore, the induced voltage increased with the applied voltage. The voltage distribution inside the tube is simulated by AC/DC model of COMSOL Multiphysics 4.3 and shown in Fig. 5(b). The peak voltage value is right below the ring electrode, so the induced voltage was larger and increased faster when part of it was moved out of the tube. On the other hand, because the voltage was measured on the copper wire inside the FDBCE, and the dielectric barrier was as the capacitor, the voltage of FDBCE was less than that of FPE.

The propagation dynamics are shown in Fig. 6 to analyze the effect of different floating electrodes on plasma jets. For the case of FPE inside the tube, the plasma first appeared as a positive corona at the end of FPE at 200 ns, which was indicated by the emission confined in the region less than 0. 3 mm from the electrode [Fig. 6(m)]. The voltage on the ring electrode and the pin electrode is 6 kV and 3.5 kV, respectively [Fig. 5]. The strong electric field due to the large voltage difference between ring electrode and pin electrode and the tip curvature $r = 20\,\mu m$ is the reason for the corona discharge. Once the corona discharge happened, positive ions accumulated on the surface of pin electrode; therefore, the voltage of FPE kept increasing [Fig. 5(a)], and the discharge inside the dielectric tube became more intense [Fig. 6(n)]. However, because the electric field between positive ions on the floating electrode and electrons accumulated on the inner surface of dielectric tube is opposite to the applied electric field, and its magnitude increased within the intense discharge inside the tube and decreased the effect of applied electric field, the intense discharge inside the tube was kept only 15 ns. Afterwards, the discharge developed along the inner surface of tube and changes into plasma bullet when it ran out of the tube. When the plasma bullet propagated towards the ground electrode, the side view picture shown in Fig. 6(o) suggests the ionization and excitation was stronger in the mixing layer of helium and air [compare Fig. 6(o) and Fig. 4(b)]. This is the typical characteristics of ring shape plasma bullet, and the end view picture taken at the same time shown in Fig. 7(c) indeed captured this plasma bullet in the ring shape.[13] The stronger ionization in the mixing layer is attributed to the lower ionization level of $N_2(E + N_2 -> 2e + N_2^+, 15.6\,eV)$ compared with that of $He(e + He -> 2\,e + He^+,\ 24.587\,eV)$ and supports the earlier simulation results.[14]

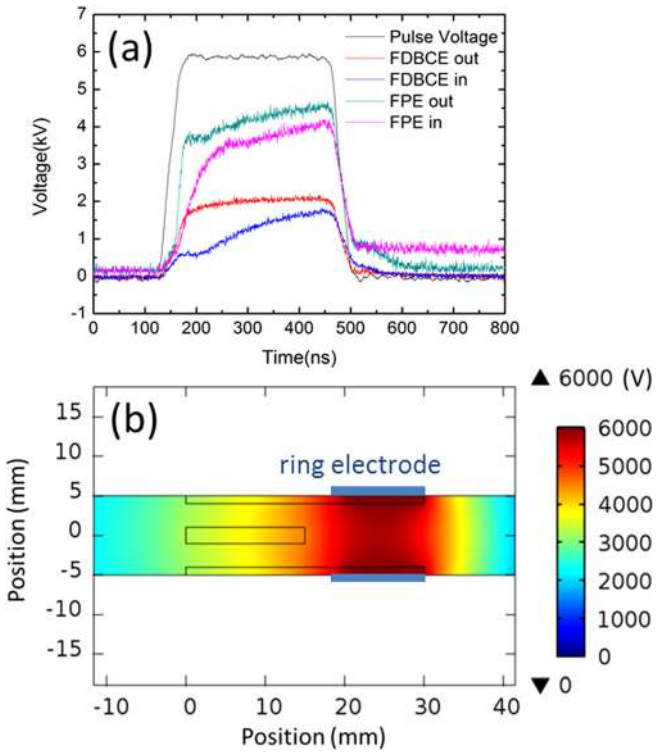

FIG. 5. (a) Electrical characteristics of pulsed DC plasma jet with FDBCE and FPE at different positions. (b) Voltage distribution inside the tube before gas breakdown.

During the following 90 ns, the plasma bullet transited from the ring shape to the disk shape. Fig. 6(p) indicates the strong ionization happened not only in the mixing layer but also in the FPE horizontal extension region with high helium concentration [Fig. 4(b)]. The end view shown in Fig. 7(d) indicates the disk shape of plasma bullet. This transition is different from the traditional constriction of ring shaped structure happened at the end of plasma bullet propagation.[15] These tradition discharge devices do not have the confinement of ground electrode at the opposite of dielectric tube, and the constriction is attributed to the diffusion of air into helium flow channel.[15–17] However, the ground electrode and 2 cm gap between the tube and ground electrode provide a high helium concentration channel in the FPE horizontal extension [Fig. 4(b)]; therefore, ionization of helium dominates the ionization reaction there.[14] Helium ionization level is higher than that of nitrogen, then the question is where the energetic electrons are from. Since the high conductivity of dark channel behind the plasma bullet, the voltage drop along plasma channel increased slowly during plasma jet propagation.[16] The electric field in the plasma bullet became stronger as the result of decreasing gap between plasma bullet and the ground electrode, which is also by the increasing 706 nm emission from the tip of plasma bullet (data now shown).[18–22] So the electrons produced by photo-ionization[13] were accelerated by this increasing electric field and ionized helium in the PE axis horizontal extension region. For the energetic electrons in the mixing layer, they are consumed not only by rotation and vibration state of N_2 and O_2 but also by attachment to O_2.[8,14] Therefore, the ionization in the high helium concentration region increased, and the plasma bullet changed from ring shape to disk shape. The larger and brighter plasma bullet shown in Fig. 6(q) suggested the effect of enhanced electric field between the propagating plasma bullet and the ground electrode again.

The transition of the plasma bullet from the ring shape to disk shape is also observed when the FDBCE is totally inside the tube [compare Figs. 6(c) and 6(d)]. Figs. 6(c)–6(e) suggest the discharge inside the tube developed backward and its velocity is only a quarter of the forward plasma bullet velocity. This emphasizes the role of air ambient in the plasma bullet formation, because the ionization photons

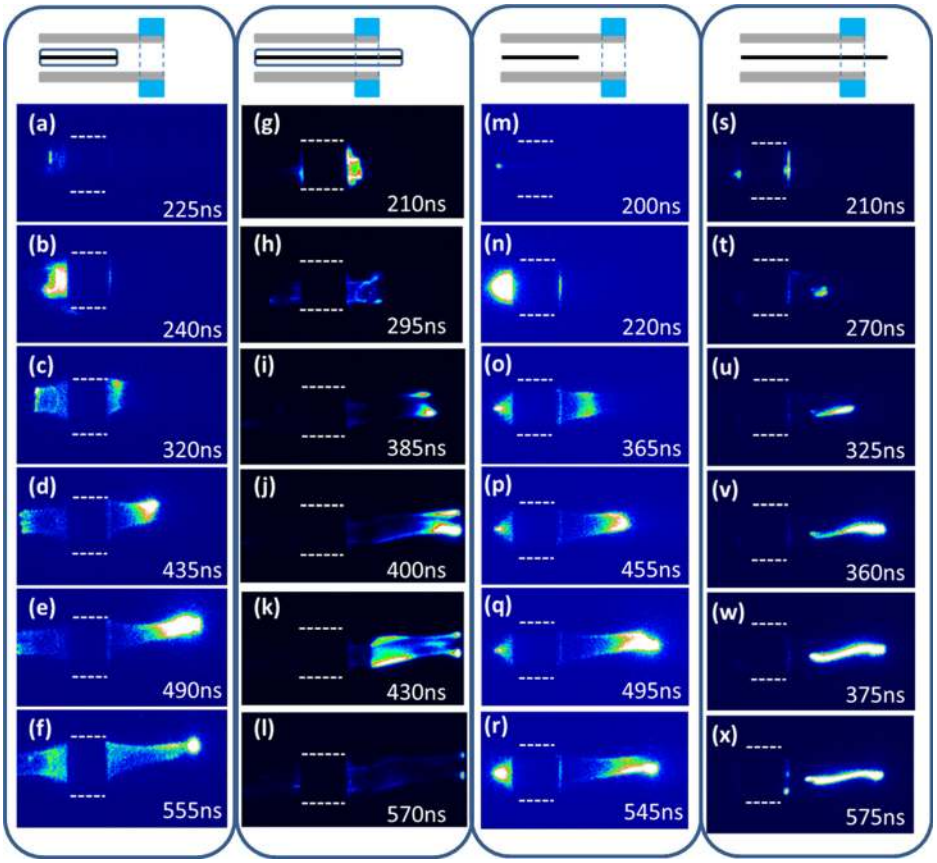

FIG. 6. The plasma jet propagation dynamics. Each image was taken with 5 ns exposure time. (a)–(f) FDBCE inside the tube, (g)–(l) FDBCE outside the tube, (m)–(r) FPE inside the tube, (s)–(x) FPE outside the tube.

emitted by N_2 which have wavelengths in the range 98–102.5 nm (~12.1–12.65 eV) and photo-ionization of oxygen molecules[14,23] guided the propagation of plasma bullet. During the pulse off period, due to the accumulated surface charge, the secondary discharge[18] happened not only between the FDBCE and inner surface of the ring electrode but also along the plasma channel to the ground electrode [Fig. 6(f)]. The similar conditions because of the secondary discharge were observed for the other three cases [Figs. 6(l), 6(r), and 6(x)].

When part of the FPE was moved out of the tube, intense discharge first happened between FPE and inner surface of dielectric tube [Fig. 6(s)], which is as the traditional dielectric barrier discharge (DBD).[24] The charges quickly spread along the FPE surface, so the strong electric field formed at the tip of FPE. Afterwards, the discharge inside the tube turns weaker, and the plasma streamer developed along the extension of FPE [Fig. 6(t)], which is in the high helium concentration region [Fig. 4(d)]. This is different from the development of plasma along the mixing layer of helium and air for the case of FPE inside tube. The actual mechanisms for this streamer propagation included the electron diffusion, the ponderomotive force, and the breakdown wave.[25,26] The time averaged plasma streamer propagation speed is 1.1×10^5 m/s, which is higher than 0.8×10^5 m/s when FPE was inside the tube. After the streamer reached the ground electrode, a stable plasma channel connected FPE and ground electrode [Fig. 6(w)], and the intense discharge increased the charge accumulation on the FPE. Therefore, the voltage on FPE is higher when part of it was moved out of the tube [Fig. 5(a)].

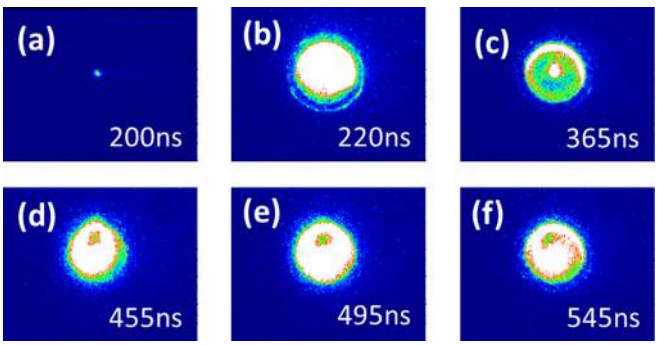

FIG. 7. The end view of plasma jet propagation for the case of FPE inside the tube. The time of (a)–(f) is same as time of side view pictures (m)–(r) in sequence. Each image was taken with 5 ns exposure time.

FDBCE also dominated the plasma jet formation when part of it was moved out of the tube. After the intense DBD between the ring electrode and FDBCE [Fig. 6(g)], two separate plasma bullet ran from the edge of FDBCE [Fig. 6(h)]. The structure and surface charge of the FDBCE are possible reasons for the formation of two separate plasma bullets. Two plasma bullets became stronger during its propagation to the ground electrode [Figs. 6(i) and 6(j)], which certified the stronger electric field between plasma bullet and ground electrode during the bullet propagation. Once the plasma bullet contacted with the ground electrode, the return stroke[27,28] quickly propagated backward to the FDBCE [Fig. 6(k)]. Its velocity is 1.5×10^6 m/s, which is an order larger than the forward velocity (~10^5 m/s). The high conductivity due to

electron density of $10^{12}/cm^3$ in the dark channel behind the plasma bullet is the reason for such a high backward velocity.[16] The fast moving return stroke was also observed when FPE was outside the tube, and it leaded to the formation of a bright plasma channel connected the FPE to ground electrode [Figs. 6(v) and 6(w)]. This bright plasma channel lasts for more than 200 ns [Figs. 6(w) and 6(x)] until all deposited charge on FPE was dissipated; therefore, a single intensified plasma jet was observed in Fig. 3(d).

IV. CONCLUSION

In conclusion, two kinds of floating electrodes were tested in this experiment. The discharge between the power electrode and floating electrodes decreased the voltage to trigger plasma jet substantially. The transition of plasma bullet from ring shape to disk shape in the high helium concentration region happened when floating electrodes were totally inside the powered ring electrode. This transition is attributed to increasing electric field between the plasma bullet and ground electrode. The double plasma bullets and single intensified plasma jet were observed when part of FDBCE and FPE were outside the powered ring electrode, respectively. The surface structure and deposited charge of FDBCE result in the formation of double plasma bullets. The return stroke which connected the FPE to the ground electrode is the reason for the single intensified plasma jet.

ACKNOWLEDGMENTS

This work was supported by the National Natural Science Foundation of China under Grant No. 51007029, the Fundamental Research Funds for the Central Universities under Grant No. 18131012, and the SRF for ROCS, SEM.

[1]F. Roman, V. Cooray, and V. Scuka, J. Electrost. **37**, 67 (1996).
[2]G. Fridman, M. Peddinghaus, M. Balasubramanian, H. Ayan, A. Fridman, A. Gutsol, and A. Brooks, Plasma Chem. Plasma Process. **26**, 425 (2006).
[3]H. W. Lee, S. H. Nam, A.-A. H. Mohamed, G. C. Kim, and J. K. Lee, Plasma Processes Polym. **7**, 274 (2010).
[4]T.-C. Tsai and D. Staack, Plasma Processes Polym. **8**, 523 (2011).
[5]Q.-Y. Nie, C.-S. Ren, D.-Z. Wang, and J.-L. Zhang, Appl. Phys. Lett. **93**, 011503 (2008).
[6]Z.-B. Wang, G.-X. Chen, Z. Wang, N. Ge, H.-P. Li, and C.-Y. Bao, J. Appl. Phys. **110**, 033308 (2011).
[7]X. Lu, Z. Jiang, Q. Xiong, Z. Tang, and Y. Pan, Appl. Phys. Lett. **92**, 151504 (2008).
[8]X. Lu, M. Laroussi, and V. Puech, Plasma Sources Sci. Technol. **21**, 034005 (2012).
[9]U. Kogelschatz, Plasma Chem. Plasma Process. **23**, 1 (2003).
[10]J. Walsh and M. Kong, Appl. Phys. Lett. **93**, 111501 (2008).
[11]E. Karakas, M. Koklu, and M. Laroussi, J. Phys. D **43**, 155202 (2010).
[12]M. Yousfi, O. Eichwald, N. Merbahi, and N. Jomaa, Plasma Sources Sci. Technol. **21**, 045003 (2012).
[13]N. Mericam-Bourdet, M. Laroussi, A. Begum, and E. Karakas, J. Phys. D **42**, 055207 (2009).
[14]D. Breden, K. Miki, and L. L. Raja, Plasma Sources Sci. Technol. **21**, 034011 (2012).
[15]Q. T. Algwari and D. O'Connell, Appl. Phys. Lett. **99**, 121501 (2011).
[16]J.-P. Boeuf, L. L. Yang, and L. C. Pitchford, J. Phys. D **46**, 015201 (2013).
[17]S. Wu, Q. Huang, Z. Wang, and X. Lu, IEEE Trans. Plasma Sci. **39**, 2286 (2011).
[18]J. T. Hu, X. Y. Liu, J. H. Liu, Z. L. Xiong, D. W. Liu, X. P. Lu, F. Iza, and M. G. Kong, Phys. Plasmas **19**, 063505 (2012).
[19]X. Y. Liu, J. T. Hu, J. H. Liu, Z. L. Xiong, D. W. Liu, X. P. Lu, and J. J. Shi, Appl. Phys. Lett. **101**, 043705 (2012).
[20]J. He, J. Hu, D. Liu, and Y.-T. Zhang, Plasma Sources Sci. Technol. **22**, 035008 (2013).
[21]D. W. Liu, F. Iza, and M. G. Kong, Appl. Phys. Lett. **95**, 031501 (2009).
[22]J. H. Liu, X. Y. Liu, K. Hu, D. W. Liu, X. P. Lu, F. Iza, and M. G. Kong, Appl. Phys. Lett. **98**, 151502 (2011).
[23]P. Ségur, A. Bourdon, E. Marode, D. Bessieres, and J. H. Paillol, Plasma Sources Sci. Technol. **15**, 648 (2006).
[24]J. J. Shi, J. Zhang, G. Qiu, J. L. Walsh, and M. G. Kong, Appl. Phys. Lett. **93**, 041502 (2008).
[25]J. Shi, F. Zhong, J. Zhang, D. W. Liu, and M. G. Kong, Phys. Plasmas **15**, 013504 (2008).
[26]A. Böhle, O. Ivanov, A. Kolisko, U. Kortshagen, H. Schlüter, and A. Vikharev, J. Phys. D **29**, 369 (1996).
[27]R. S. Sigmond, J. Appl. Phys. **56**, 1355 (1984).
[28]K. Ostrikov, E. C. Neyts, and M. Meyyappan, Adv. Phys. **62**, 113 (2013).